To appear in Proceedings of the NASA Conference on Space Telerobotics, Jan. 31 - Feb. 2, 1989, Pasadena, CA.

TECHNOLOGY AND TASK PARAMETERS RELATING TO THE EFFECTIVENESS OF THE BRACING STRATEGY

Wayne J. Book, J. J. Wang

The George W. Woodruff School of Mechanical Engineering
Georgia Institute of Technology
Atlanta, Georgia 30332

1. Introduction

The bracing strategy has been proposed in various forms [1] as a way to improve robot performance. One version of the strategy employs independent stages of motion. The first stage, refered to here as the large or bracing arm, carries the second stage of motion. After the first stage has completed its motion it is braced to provide a more rigid base of motion with a more accurate relationship to the parts to be manipulated. The hypothesis of this research is that more rapid completion of certain tasks is possible with lighter arms using the bracing strategy. While it is easy to make conceptual arguments why this should be so, it is less easy to specify even approximately when this will be true for some reasonably generic situation. There is no relevant experience base with bracing arms to be compared to non-bracing arms. Furthermore, if one were interested in obtaining such practical, or at least relevant, experience, there would be no methodical guidance on the selection of an interesting case.

An "interesting case" is one in which the unproven approach, bracing in this paper, can show its superiority. If one such case exists, only the extent of applicability of the new approach is in question. One set of "interesting cases" is likely to be applications in which a large workspace must be covered, but where a series of small accurate moves will remain within a smaller region of the total workspace. A prototype application with these characteristics will be set up and a skeleton design of arms using the competing strategies will be compared.

2. The Problem Studied

This paper compares two operational and design strategies to pick and place a stack of n parts as depicted in Fig. 1. The first strategy employs a single arm l_1 which moves through an initial distance d_m to the part location. It then repeatedly moves a distance d_p to relocate the n parts at the final location. The second strategy employs two arms. The first arm of length l_2 carries the second arm to a bracing position from which a second short arm of length l_s to a bracing position from which the short arm can complete the n part relocation moves. The question to be answered is: Under what combinations of task parameters, technology capabilities and performance measures should one consider the bracing strategy.

The most relevant task parameters seem to be the distance of the initial move, D_m, the distance of the repeated moves, D_p the number of repeated moves n, the payload mass mp, and the size of the workspace to be covered, represented by a length of the single arm, l_1. The task chosen is also representative of other tasks in which operation is concentrated for a time within a small region of the total workspace.

The performance measures examined are the time to complete the task and the weight, under certain constraints to be described later.

The level of technology employed affects the study in several ways. The elastic modulus, maximum stress, and material density are three parameters of the material technology, for instance. These are held constant in the results presented here at values found in common engineering materials, in this case aluminum. The structural technology combines the material parameters and the task parameters to determine structural natural frequencies, mass moments of inertia, and stress. The structural technology represented here is a Bernoulli-Euler beam with a

uniform hollow circular cross section. The control technology is represented by the bandwidth of the fine motion control as a fraction of the lowest structural frequency. While advanced control schemes can now achieve higher fractions, this study assumes fine motion bandwidth of 1/2 of the first structural frequency when the joints are clamped as is representative of the limits of standard joint PID control of actuator torque. Gross motion is assumed to be limited only by the actuators and the load inertia, both of which are based on structural strength. The actuator technology represented here is the moving coil d.c. motor with a gear reduction. The motor is chosen for minimal weight to meet the peak power demands and the reducer is chosen based on required output torque.

Complete, multi-degree of freedom arm designs would be convincing to the reader in making this comparative study. However, it would be extremely time consuming and would involve an immense number of irrelevant and distracting decisions. The current study involves a far simpler design intended to capture the essence of the realistic case. The results are qualitatively applicable to real arms and can hopefully be calibrated with existing complete designs. Each arm is represented by a single beam and a single joint. For the bracing case, the large arm and the small arm it carries are each represented by a single link.

List of Symbols

a_{max} : Maximum arm acceleration
D_a : Positioning accuracy
D_m : Distance of large move between task areas
D_p : Distance of small move for fine tasks
d : Arm diameter
d_s : Short arm outside diameter in bracing strategy
d_1 : Nonbracing single arm OD
d_2 : Bracing arm in bracing strategy
E : Young's Modulus
I : Area moment of inertia
J : Moment of inertia of arm with payload
K_p : Position feedback gain in fine motion control
K_r : Ratio of arm inner and outer diameter
l : Arm length
l_s : Short arm length
l_1 : Nonbracing arm length
l_2 : Bracing arm length
M_d : Harmonic drive weight
M_m : Motor weight
M_s : Short arm system weight
m_p : Payload mass
n : Number of parts to be moved
P_{max} : Maximum motor power required in task motion
P_{fmax} : Maximum motor power required in fine motion
P_{gmax} : Maximum motor power required in gross motion
s : Fatigue strength of arm material
T_{qmax} : Maximum torque allowed
t_f : Fine motion time
t_g : Gross motion time
t_t : Total task time
θ_a : Fine motion range of arm with payload at the end point
θ_f : Fine motion range of the task
θ_g : Gross motion range of the task
θ_t : Complete task range
u : Arm mass per unit length
V_{imax} : Arm initial velocity entering fine motion range

V_{fmax} : Maximum arm velocity in fine motion
V_{gmax} : Maximum arm velocity in gross motion
W_c : First natural frequency of clamped arm
W_s : Servo bandwidth of fine motion feedback control system

3. Fine Motion and Gross Motion of a Single Link Arm

In both the bracing and nonbracing strategies the proposed task is accomplished through a series of single link moves. Task completion time is the accumulation of time for these single link moves. As a basis for the evaluation of proposed task performance, a general single link motion is first defined and analyzed. The results will then be utilized for the performance comparison of bracing and nonbracing strategies.

General arm motion can be considered as a combination of fine motion and gross motion [2]. Fine motion is defined as that part of the complete task motion commanded by the a linear feedback control law to move the arm joint to the desired position with a certain accuracy. This fine motion therefore occurs only within a certain range, which is called fine motion range, θ_f which is determined by the actuator capacity and feedback control law. Motion outside this fine motion range is called gross motion. Gross motion thus precedes fine motion and gross motion range is the whole desired task motion range, θ_t less fine motion range. It is obvious that depending on the range of the task, gross motion might not be required. To reduce task time, it would be desirable to move through the complete gross motion region as fast as possible using the maximum available torque and then in the fine motion range let the feedback control lead the arm to its final position with the specified accuracy.

Gross motion in this study is designed so that arm is accelerated and decelerated with maximum motor torque T_{qmax}. By virtue of light weight arm design and neglecting the gravity force, T_{qmax} is determined by s, the arm material fatigue strength for infinite life cycle. For a circular arm cross section of outside diameter d, area moment of inertia I, the maximum allowed torque:

$$T_{qmax} = \frac{2Is}{d} \tag{1}$$

The fine motion feedback control law in this study is linear PD control which uses joint position and velocity feedback with final desired position as a step input. The resulting system performance will be evaluated as a second order linear system. With only the joint variables available to the controller, flexibility inherent in a light weight arm generally will cause difficulty in maintaining end point position accuracy. To provide fast arm joint response and at the same time be able to damp out and avoid exciting flexible vibration, a general design criteria [3] suggests that system servo bandwidth ω_s be chosen to be half of the first clamp-free natural frequency ω_c of the arm with payload attached. An approximation for the first natural frequency is given by Den Hartog [4]:

$$W_c = \sqrt{\frac{EI}{l^3(0.23ul+mp)}} \tag{2}$$

where E: Young's modulus
l: Arm length
u : Arm mass per unit length
m_p: Payload mass

System servo bandwidth W_s is determined by position feedback gain K_p and system total inertia J and is set to be $W_c/2$.

$$W_s = \sqrt{\frac{K_p}{J}} = \frac{W_c}{2} \tag{3}$$

Based on the fine motion definition above, fine motion range for the arm with payload is:

$$\theta_a = \frac{T_{qmax}}{K_p} \tag{4}$$

Substituting (1) and (3) into (4), θ_a can be expressed as a function of arm characteristics and payload:

$$\theta_a = \frac{8sl(0.23ul+m_p)}{Ed(1/3ul+m_p)} \tag{5}$$

When payload mass m_p is much larger than arm mass, Eq. (5) can then be reduced to:

$$\theta_a = \frac{8sl}{Ed} \tag{6}$$

Arm fine motion range is shown to be only a function of material properties s, E and arm slenderness ratio l/d.

Arm fine motion range θ_a is a characteristics of the combined arm structure and payload. Depending on the task and the arm used, the task fine motion range θ_f might be equal to or smaller than θ_a. If the task range θ_t is larger than arm fine motion range θ_a, the task fine motion range will be $\theta_f=\theta_a$ and the gross motion range will be $\theta_g=\theta_t-\theta_a$. On the other hand, if θ_t is less than or equal to θ_a, the fine motion range will be $\theta_f=\theta_t$ and gross motion will not be required. To illustrate this, a single arm task is shown in Fig 2 , where a payload of 60 lb is to be moved a linear distance of 3 ft by an arm of fixed cross section for various arm lengths. The task range here is the angle the arm has to move to accomplish the task. The results show how the task range θ_t, task fine motion range θ_f, task gross motion range θ_g and arm fine motion range θ_a vary as functions of the arm length. The gross motion range decreases rapidly with longer arm since task range gets smaller and the arm fine motion range increases.

4. Fine Motion and Gross Motion Time

With the gross motion and fine motion and their control strategies defined above, performance time for each task move can be evaluated.

To avoid overshoot and achieve fast response in fine motion, the second order linear system of fine motion is set to have critical damping. For an arm to move θ_f, $\theta_f <= \theta_a$ to within an end point accuracy of D_a with θ_f as a step input, the fine motion time t_f:

$$\ln(D_a/l) = \ln(\theta_f + (\theta_f * W_s - V_i) * t_f) - W_s * t_f \tag{7}$$

where

V_i: Arm initial velocity of fine motion. $0 <= V_i <= \theta_a * W_s$

V_i is equal to zero when gross motion is not required for the task and the arm will start the fine motion from rest. Larger fine motion initial velocity, which is also the gross motion end velocity, will certainly reduce gross and fine motion time. However, it is limited by $V_{imax}=\theta_a * W_s$ to ensure that overshoot will not occur and the fine motion control torque will remain within T_{qmax} during the transition from gross motion bang-bang control to fine motion feedback control.

Depending on the gross motion range θ_g, gross motion will fall into one of the three categories discussed below:

1): $\theta_g < (1/2) * V_{imax}^2 / a_{max}$, $a_{max} = T_{qmax}/J$

This indicates that gross motion range is too small for the arm to accelerate to the maximum allowed fine motion entry velocity. Step changes in applied torque result in two jerks (bang-bang) as shown in the velocity profile, Fig

3A and 3B at one point where gross motion starts and the other point where the transition from gross motion to fine motion occurs. Fig 3A is for the case where $\theta_g < 1/8*V_{imax}^2/a_{max}$ and acceleration continues after switching into fine motion control. Fig 3B is for the case where $1/8*V_{imax}^2/a_{max} <= \theta_g < 1/2*V_{imax}^2/a_{max}$ and fine motion starts with deceleration.
Gross motion time t_g:

$$t_g=(2*\theta_g/a_{max})^{1/2} \tag{8}$$

Maximum arm velocity V_{gmax}:

$$V_{gmax}=(2*a_{max}*\theta_g)^{1/2} \tag{9}$$

2): $\theta_g >= (1/2)*V_{imax}^2/a_{max}$

This is the case where the arm is able to reach the velocity V_{imax} within gross motion range. Deceleration is required to reduce the velocity to V_{imax} when the arm enters the fine motion range. As in previous case, two step changes in applied torque are experienced with one at the start of gross motion while the other at the point when maximum reverse torque is applied to decelerate the arm to prepare for the fine motion, Fig 3C. There is no jerk at the transition from gross motion to fine motion since the fine motion control also commands a maximum reverse torque at this point due to the choice of maximum fine motion initial velocity, $V_{imax}=\theta_f*W_s$.
Gross motion time t_g:

$$t_g=(4*\theta_g/a_{max}+2*V_{imax}^2/a_{max}^2)^{1/2}-V_{imax}/a_{max} \tag{10}$$

Maximum arm velocity V_{gmax}:

$$V_{gmax}=(t_g+V_{imax}/a_{max})*a_{max}/2 \tag{11}$$

3): $\theta_g=0$

Gross motion is not required when task range is smaller than the arm fine motion range. Fine motion will have zero initial velocity, Fig 3D. One jerk exists at the start of the motion.

The total time T_t for each task move is the sum of T_f and T_g:

$$t_t=t_g+t_f \tag{12}$$

5. System Weight

System weight is the total of arm, motor and reduction gear drive weight. It is also considered as a measure of performance comparison for different arm designs. Motor technology is represented here by DC moving coil motor and a harmonic drive is chosen as reducing gear component. Neglecting motor and harmonic drive inertia, an equation to calculate DC moving coil motor weight M_m is approximated by Sangveraphunsiri [5]:

$$M_m=P_{max}/50 \text{ lb} \tag{13}$$

P_{max} is the larger of maximum power required for gross motion, P_{gmax} and fine motion P_{fmax}.

$$P_{gmax}=T_{qmax}*V_{gmax} \tag{14}$$

$$P_{fmax}=T_{qmax}*(\theta_f/\theta_a)*V_{fmax} \tag{15}$$

where $T_{qmax}*(\theta_f/\theta_a)$ is the maximum torque commanded in fine motion by feedback control.

By fitting typical harmonic drive data, its weight M_d as a function of torque can be calculated according to:

$$M_d = \frac{*T_{qmax}*\theta_f/\theta_a)^{1.027}}{467.735}$$

6. Single Arm Performance Analysis

The above quantitative gross and fine motion characterization of arm motion will serve as the basis for the following analysis of task performed by arms of different design.

The same task described earlier will be used again here. Referring to the schematic in Fig 2, an arm of circular cross section with the ratio of inner to outer diameters, K_r=0.9 is required to move 3 ft a payload of 60 lb.

Fig 4 and 5 show how the task completion time and system weight change as function of arm length for several arm OD's. A break down of task time is shown in Fig 6 for the case of OD=2 in. Notice the correspondence between this figure and Fig showing the gross/fine motion range of the same structure and task. It is clear from these figures that a shorter arm of fixed OD has better time performance but greater total weight since greater speed and torque are used. The time performance of a more rigid arm (larger OD) is better and less affected by arm length than that of a lighter arm, however, at the cost of greater system weight, especially for the short length arms.

Another way to analyze system performance is to impose the task time requirement for each arm of various length and see how the arm OD, motor and gear reducing components will vary to meet the different time requirements. For the same previous task, the results are shown in Fig 7 and Fig 8 for the task time of 1, 2 and 3 seconds. A breakdown of system weight is presented for the task time of 2 sec in Fig 9. For any specified task time the shorter length arm requires lower system weight. Although this advantage is not quite obvious for t=2, or 3 sec, where lighter arms are used, it gets quite significant as task time is further reduced to 1 sec or less.

It can be concluded from the above analysis that a shorter arm is more effective in both time performance and total weight. Although detailed examination shows that the most effective arm length is not the shortest that can reach both points but almost the shortest, it is still fairly accurate to say that for a given task the best arm has a length of half task distance D_p with an OD dictated by the specified task time.

It would be useful to know how task time changes with variations of OD given the best arm length, $l=D_p/2$ so that task time can be reasonably specified. Fig 10 shows the task time as a function of arm OD with task distance D_p as a parameter and $l=D_p/2$. For small D_p (D_p=2 ft, l=1 ft), ODs of 1 to 2 in. yield about the same time performance as heavier arms but with much lower system weight required as shown in Fig 11. As D_p gets large (D_p=16 ft, l=8 ft), ODs of 1 to 2 in. become too flexible and result in poor time performance while larger OD (OD=3 in.) provides significant time improvement without much penalty in system weight. An arm designer therefore will have to carefully evaluate the trade-off between arm OD, system weight and task time specification.

The effects of positioning accuracy, D_a and payload mass, m_p are shown in Fig 12. Arms of shorter length and larger OD are less affected by payload variation and accuracy requirement.

7. Bracing Strategy in Large Work Space

As the study of single arm performance suggests, an arm with a length of half the task distance is the most effective. However, there are cases where it is neither practical nor possible to station a robot arm at the desired location. One of such cases, as mentioned in the beginning of this paper, is when the major task areas of D_p are within a large work space and separated from each other a distance of D_m (Fig 2). The major fine task here is doing n moves of distance D_p with payload of m_p as described before. Using a single arm which is long enough to move between the task areas and perform the fine task within each task area is certainly not an efficient design for the fine task. Bracing strategy suggests that the optimum arm design can still be applied to achieve the best fine task performance if a bracing arm is provided to move the short arm to its desired location and brace it to a rigid surface to do the fine task. Given equal system weight, the short arm will certainly outperform the single

nonbracing arm as found in the single arm analysis. However, bracing strategy carries some penalties. For the purpose of this study, penalties are mainly that bracing takes extra time and bracing arm and its associated motor and drive increase overall system weight with the fact that they are only utilized once for every n fine task moves.

Techniques similar to those used for the single arm performance analysis will also be used here to compare the performances of bracing and nonbracing strategies. Task time for nonbracing strategy is the total time of one large move of D_m and the sequential n small moves of D_p performed by a single arm of length l_1. For bracing strategy, task time is the sum of the time for 1) one large move of D_m by bracing arm of length l_2 with weight of short arm system M_s as its payload, 2) the bracing action, which is assumed to complete in one servo cycle of bracing arm system with payload M_s, and 3) n small moves of D_p by short arm of length l_s. The total system weight for each arm of l_1 , l_2 and l_s is calculated as in single arm analysis.

The first comparison will take l_1=15 ft, m_p=60 lb, D_p=3 ft with a bracing arm outer diameter d_2=3 in. Bracing arm length l_2 will depend on l_s according to the configuration shown in Fig 1. Fig 13 shows how the bracing and nonbracing task time changes as a function of l_s with short arm OD, d_s and n as parameters assuming both systems being equal weight for each l_s. Although a short arm of d_s=3 in. combined with bracing arm, system A performs fine task better than that of system B with d_s=2 in., system A requires much greater short arm system as shown in Fig 14 and thus its bracing arm has poor bracing motion and action performance. Therefore, bracing strategy with system A will not perform as well as with system B for small n, especially in the smaller d_s range. Fig 15. Larger n will make system A more effective as its fine task capability is more utilized, Fig 16. A plot of ratio of nonbracing and bracing task time is shown in Fig 17. As n gets larger, bracing becomes more advantageous for both system A and B and the optimal l_s moves toward left indicating a shorter short arm is more effective for larger n. In the extreme case where n is quite large and bracing becomes insignificant, the result should agree with that of single arm analysis which has that the optimal l_s is equal to half the task distance D_p.

The next comparison uses the same task and the same arm structure with d_s=2 in. and d_2=3 in. but with a smaller work space, l_1=10 ft. Its performance, task time ratio shown in Fig 18 is compared with that of l_1=15 ft. Bracing strategy is seen not as effective as in a large work space since the single arm in the nonbracing strategy can have shorter length and therefore will perform better.

Let the short arm for the fine task be chosen having l_s=1/2*D_p=1.5 ft and d_s=2 in.. Fig 19 shows that there exists an optimum bracing arm OD, d_2 for each n. As n gets larger, optimum d_2 becomes smaller. This is due to the fact that bracing arm is not often utilized so that it does not have to be as rigid as optimum bracing arm for smaller n.

8. Conclusion

Gross motion range and fine motion range are defined and equations for task time are given to evaluate a single arm task performance. They are derived under the control strategy that bang-bang control is used for the gross motion, and the fine motion is approximated by a critically damped second order linear system with PD joint variable feedback control. For a simple pick-and-place task, an arm is found to be most effective when its length is half the task distance and its diameter can be determined based on task time requirement or system weight constraint.

Bracing strategy is analyzed as sequential single arm tasks, bracing arm motion and short arm task motion, with techniques similar to those used in single arm performance analysis. Bracing strategy is advantageous over nonbracing strategy under some combinations of task parameters and bracing arm and short arm characteristics, especially in large work space and for large number of part moves, n. n is shown to have significant effect on the optimal choice of short arm and bracing arm structures for bracing strategy.

9. Suggestions for Further Research

The following are areas which can be probed based on the results of this study to gain further understanding of effectiveness and practicality of bracing strategy for any type of task in any environment.

1. Cost measures: Including not only time performance and system weight but also cost of design, manufacturing and maintenance of system for bracing strategy.

2. Gravitational effects: examining end point deflection, reduced arm strength due to gravity force and their effects on bracing strategy.

3. Optimization of short arm length for tasks which are evenly distributed within the large work space.

4. Examining tasks which require path control such as painting and welding to see how different types of tasks will affect arm structure requirement and the bracing strategy.

This work was partially supported through the Computer Integrated Manufacturing Systems program at Georgia Tech.

10. REFERENCES

1. Book, W. J., S. Le, and V. Sangveraphunsiri, "Bracing Strategy for Robot Operation," Proc. of Ro Man Sy '84 The Fifth CISM-IFToMM Symp. on Theory and Practice of Robots and Manipulators, Udine, Italy, June, 1984, pp. 179-185.

2. Book, W.J., "Characterization of Strength and Stiffness Constraints on Manipulator Control", Theory and Practice of Robots and Manipulators, A. Morecki and K. Kedzior, eds., Elsevier North-Holland, Inc, 1977, pp. 37-45.

3. Centikunt, S., Book, W.J.,"Performance of Light Weight Manipulators Under Joint Variable Feedback Control: Analytical Study of Limitations", Proc. of the 1988 American Control Conference, June 15-17, 1988, Atlanta, Georgia, pp. 1021-1028.

4. Den Hartog, J.P., Advanced Strength of Materials, McGraw Hill, 1952.

5. Sangveraphunsiri, V., W. Book and S. Dickerson, "Considerations in Selection of DC Motors for Lightweight Arms," Proc. 1984 ASME Computers in Engineering Conference, Las Vegas, NV, June 1984.

To appear in Proceedings of the NASA Conference on Space Telerobotics, Jan. 31 - Feb. 2, 1989, Pasadena, CA.

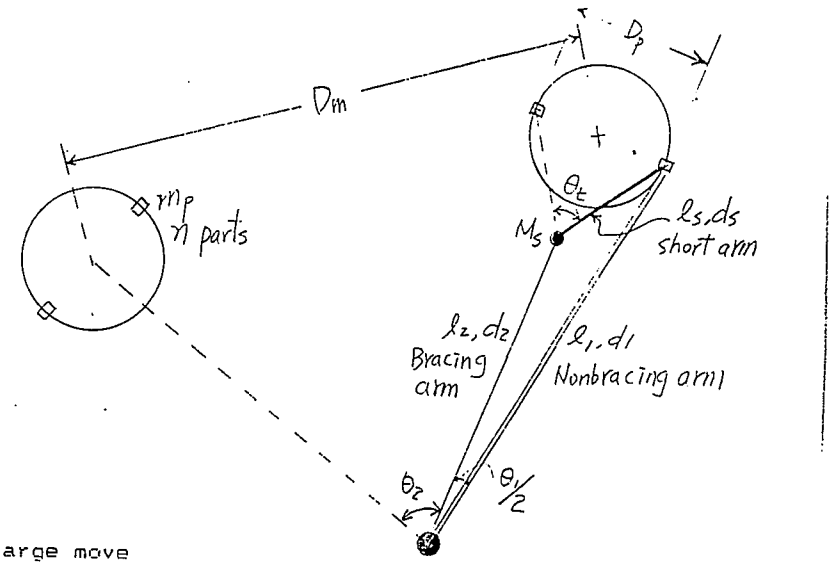

Fig. 1. Problem Task.

Task parameters:
- D_m: Distance of large move
- D_p: Distance of fine task move
- D_a: Positioning accuracy
- m_p: Payload mass
- n : Number of parts to be moved
- T : Time specification

Technology parameters:
- Material: (Aluminum)
  - E: Young's modulus
  - s: Fatigue strength s=0.002*E
  - ρ: Density
- DC moving coil motor:
  - M_m: motor weight, M_m=10.93*HP
- Harmonic drive:
  - M_d: Harmonic drive weight, $M_d=(T_{amax}*\theta_r/\theta_a)^{1.027}/467.735$
- Control:
  - Second order linear PD joint feedback control with ζ=1, $W_a=0.5W_c$

Performance measures:
- Task completion time: T_t
- System weight: M

Arm structures:
- l_a: Short arm length
- d_a: Short arm OD
- l_2: Bracing arm length
- d_2: Bracing arm OD
- l_1: Nonbracing arm length
- d_1: Nonbracing arm OD
- K_r: ID/OD=0.9
- M_a: Short arm system weight
- M_b: Bracing system weight
- M_n: Nonbracing system weight

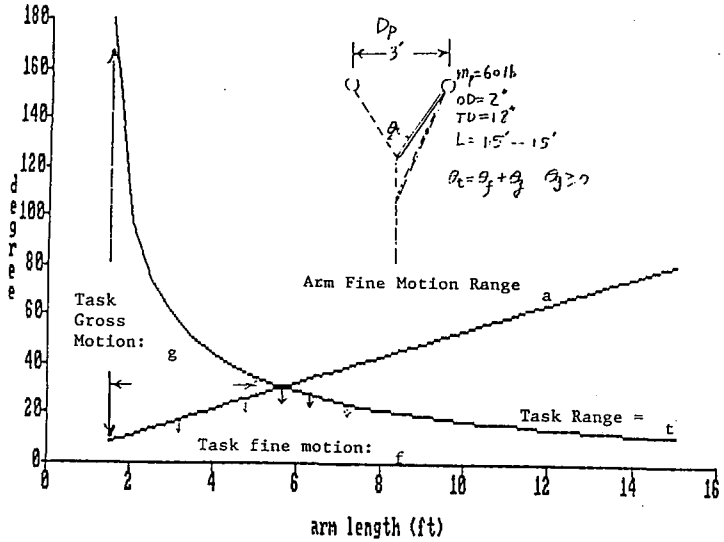

Fig. 2. Example task for a single arm: gross and fine motion range.

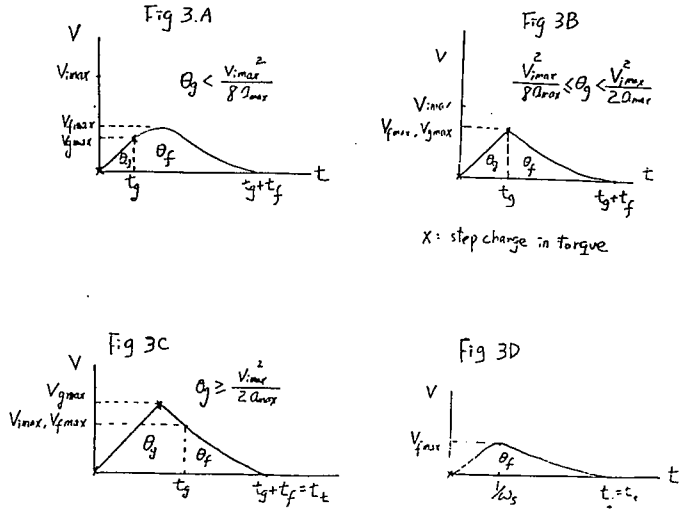

Fig. 3. Fine motion switching conditions for three cases.

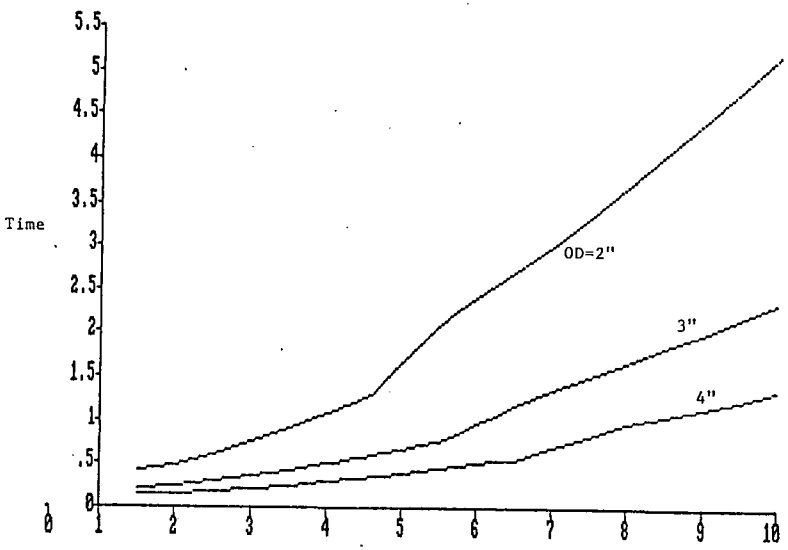

Fig. 4. Total task time for the one link case of Fig. 2.

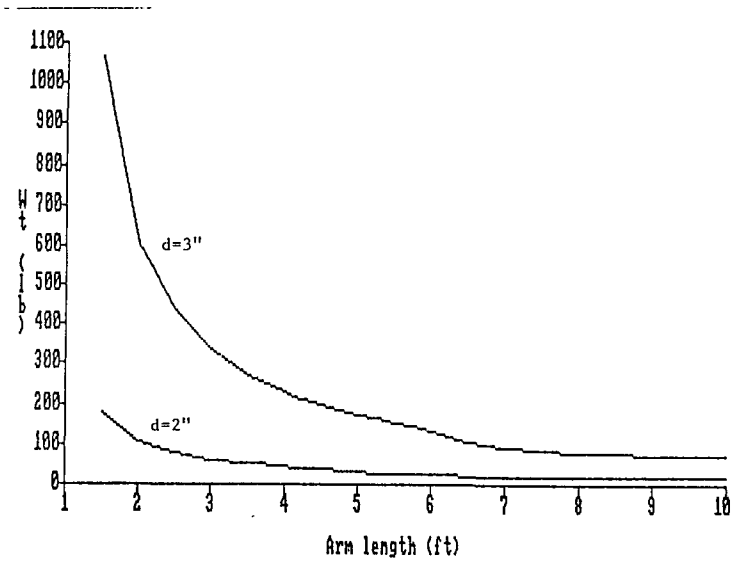

Fig. 5. Total weight for the one link case of Fig. 2.

To appear in Proceedings of the NASA Conference on Space Telerobotics, Jan. 31 - Feb. 2, 1989, Pasadena, CA.

To appear in Proceedings of the NASA Conference on Space Telerobotics, Jan. 31 - Feb. 2, 1989, Pasadena, CA.

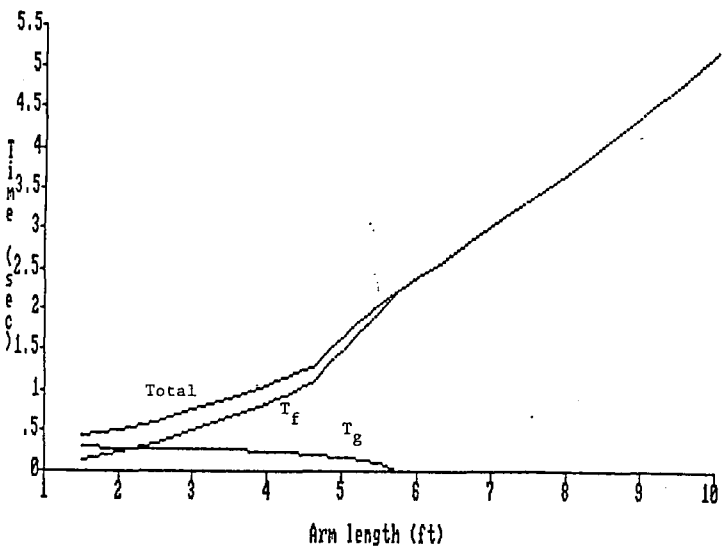

Fig. 6. Task time components for the case of Fig. 2.

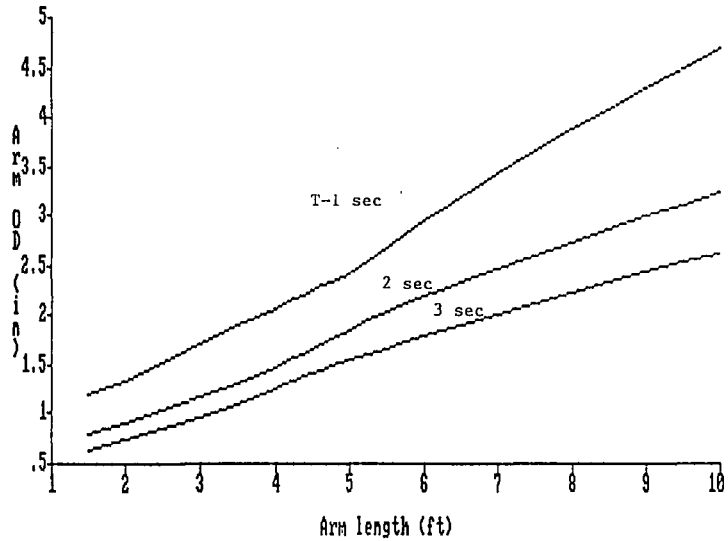

Fig. 7. Fixed task time T imposed on the one line case of Fig. 2.

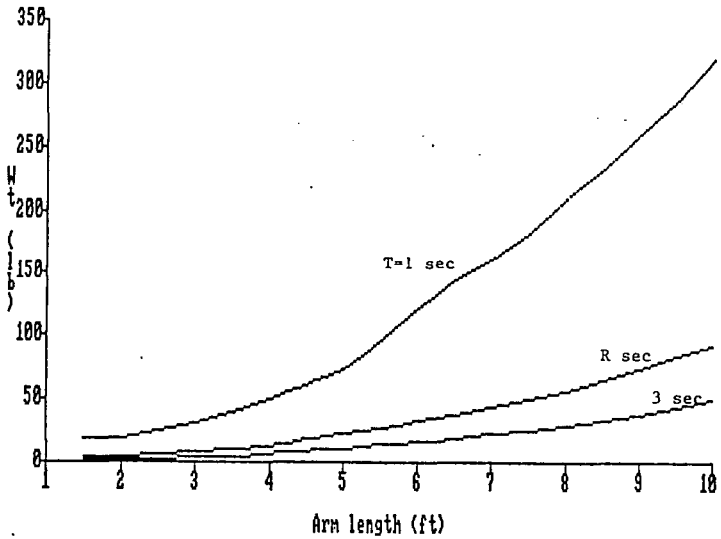

Fig. 8. Total system weight for fixed task time for the one link case of Fig. 2.

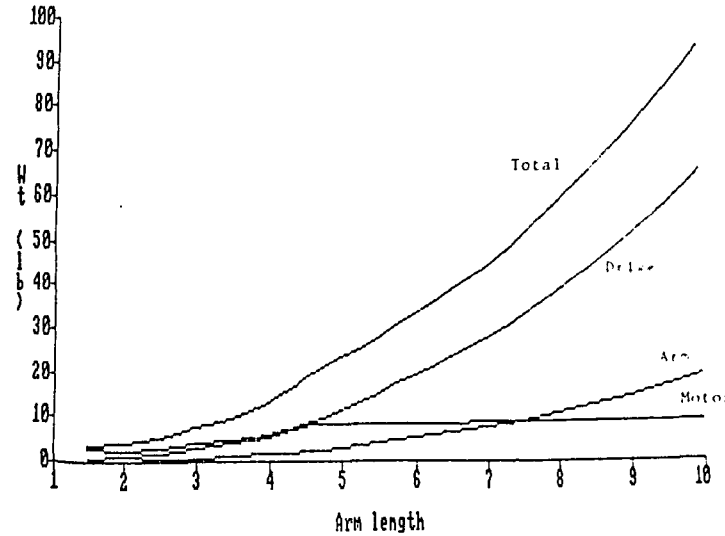

Fig. 9. System weight by component for fixed task time of 2 sec. for the one link case of Fig. 2.

To appear in Proceedings of the NASA Conference on Space Telerobotics, Jan. 31 - Feb. 2, 1989, Pasadena, CA.

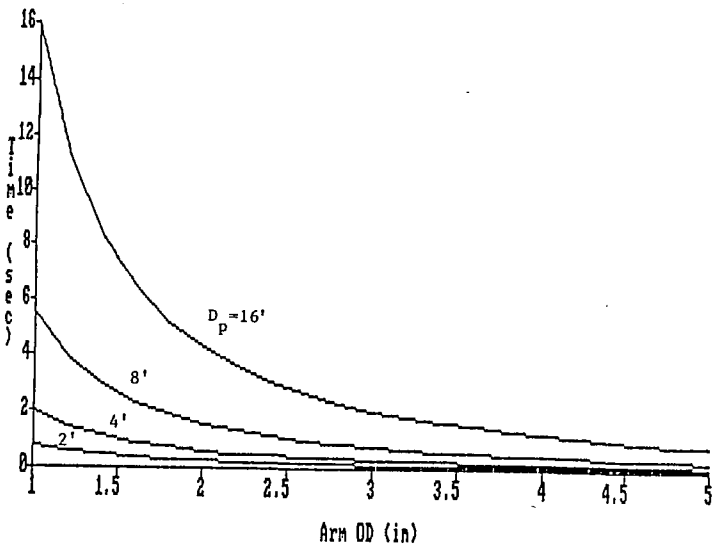

Fig. 10. Task time for fixed short arm length = $D_p/2$. (Task of Fig. 2)

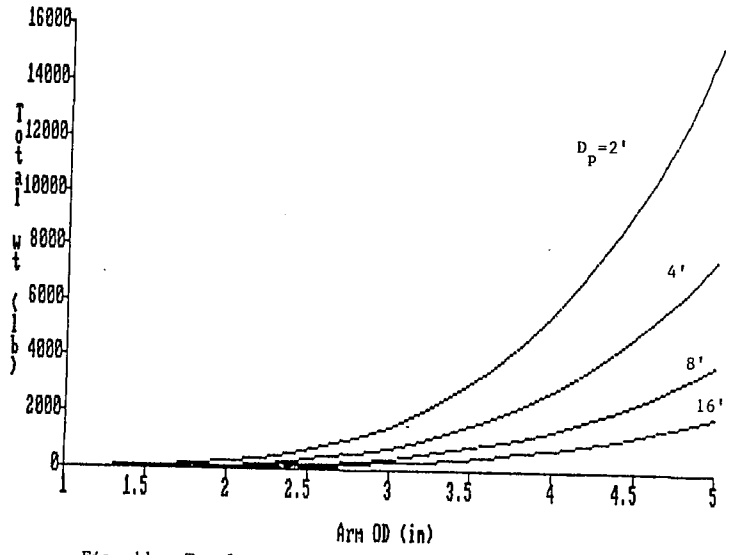

Fig. 11. Total system weight corresponding to Fig. 10.

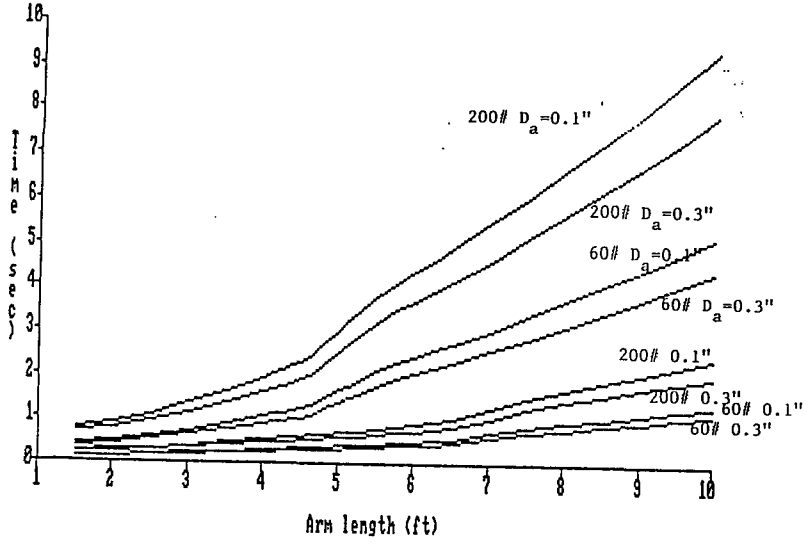

Fig. 12. Sensitivity of task time to task parameters: payload M_p and accuracy D_a. (task of Fig. 2.)

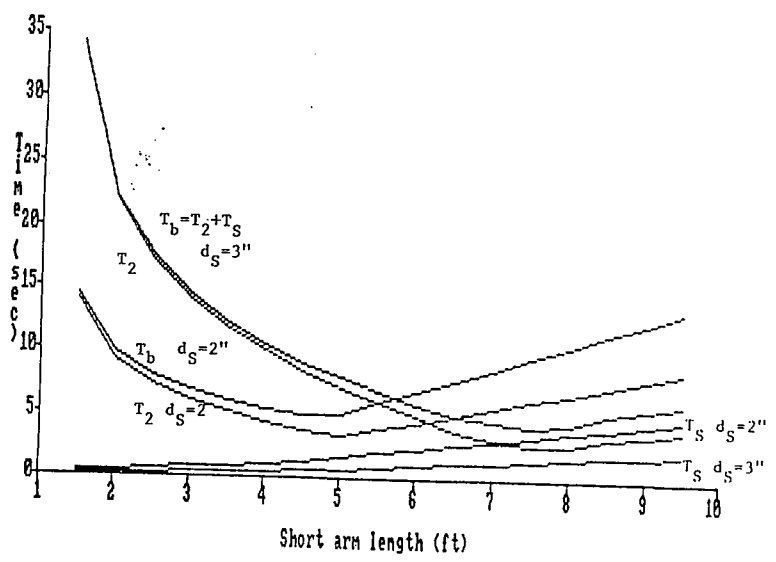

Fig. 13. Task time components T_2 and T_S for the bracing strategy for two short arm diameters, d_S. l_1 = 15', D_p=3". (See Fig. 1).

To appear in Proceedings of the NASA Conference on Space Telerobotics, Jan. 31 - Feb. 2, 1989, Pasadena, CA.

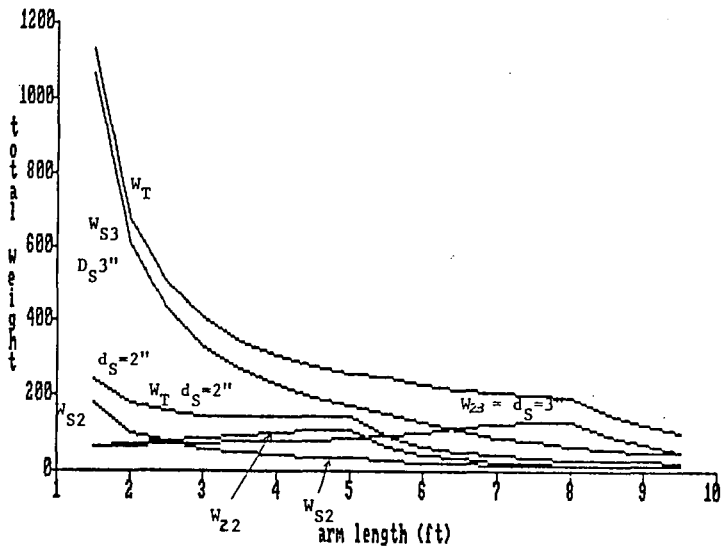

Fig. 14. Weight by component for the case of Fig. 13.

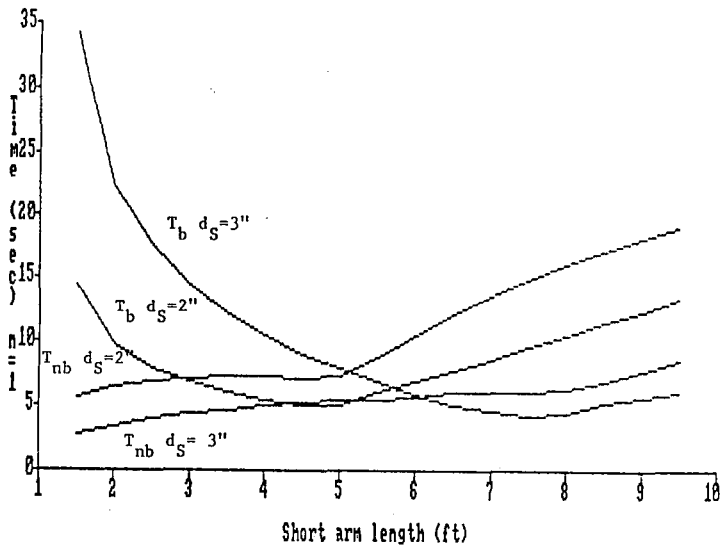

Fig. 15. Task time compared for bracing and non-bracing. (n=1)

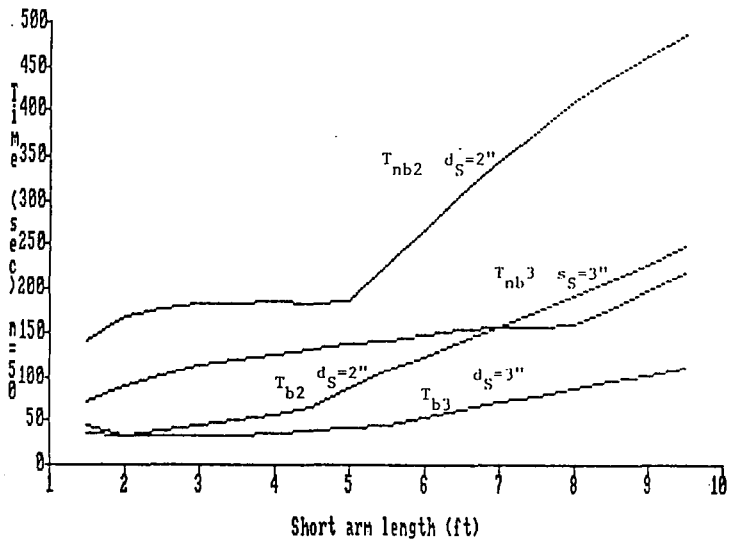

Fig. 16. Task time compared for bracing and non-bracing, (n=50).

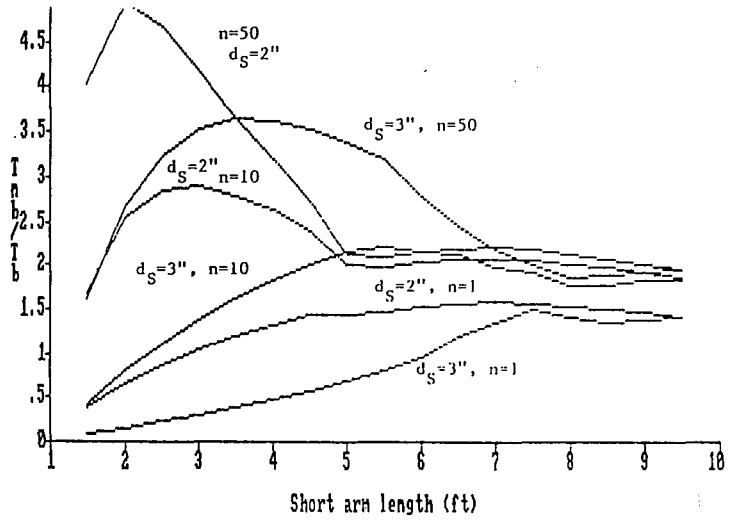

Fig. 17. Ration of non-bracing to bracing task times. (Case of Fig. 13.) l_1=15'.

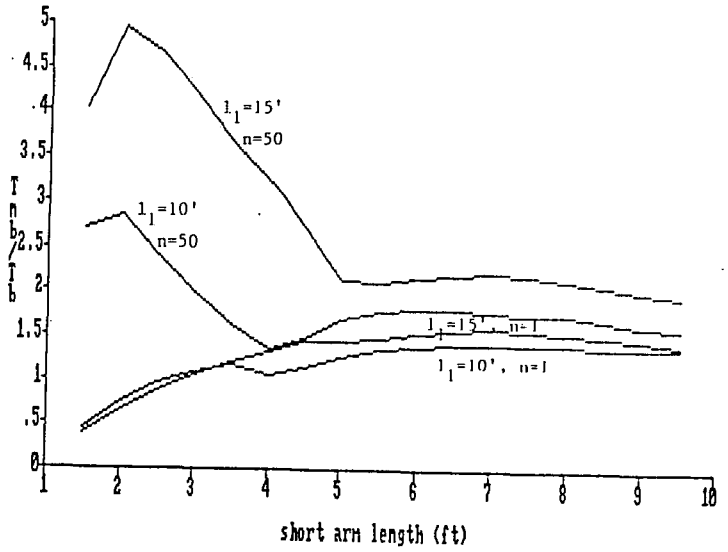

Fig. 18. Ratio of non-bracing to bracing task times. (Case of Fig. 13). l_l=10'.

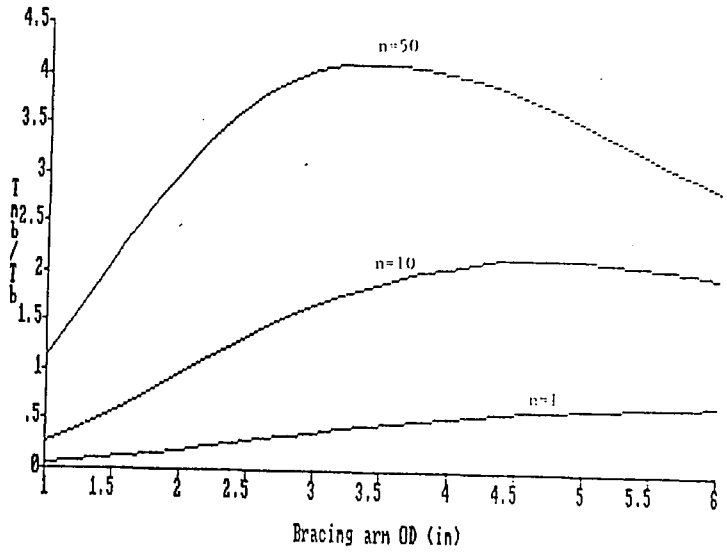

Fig. 19. Optimal bracing arm OD for a fixed short arm configuration of $l_s = D_p/2 = 1.5'$, d_s=2", l_l=15', m_p = 60 lbs.

To appear in Proceedings of the NASA Conference on Space Telerobotics, Jan. 31 - Feb. 2, 1989, Pasadena, CA.